[3]Stolz, S., Adams, N. A., and Kleiser, L., "An Approximate Deconvolution Model for Large-Eddy Simulations of Compressible Flows and Its Application to Shock-Turbulent-Boundary-Layer Interaction," *Physics of Fluids*, Vol. 13, No. 10, 2001, pp. 2985–3001.

[4]von Kaenel, R., Adams, N. A., Kleiser, L., and Vos, J. B., "The Approximate Deconvolution Method for Large-Eddy Simulation of Compressible Flows with Finite Volume Schemes," *Journal of Fluids Engineering*, Vol. 125, No. 2, 2003, pp. 375–381.

[5]Swanson, R. C., and Turkel, E., "Artificial Dissipation and Central Difference Schemes for the Euler and Navier–Stokes Equations," AIAA Paper 87-1107, Jan. 1987.

[6]Vos, J. B., Rizzi, A. W., Corjon, A., Chaput, E., and Soinne, E., "Recent Advances in Aerodynamics Inside the NSMB (Navier–Stokes Multi-Block) Consortium," AIAA Paper 98-0225, Jan. 1998.

[7]Coleman, G. N., Kim, J., and Moser, R. D., "A Numerical Study of Turbulent Supersonic Isothermal-Wall Channel Flow," *Journal of Fluid Mechanics*, Vol. 305, 1995, pp. 159–183.

[8]Lenormand, E., Sagaut, P., Ta Phuoc, L., and Comte, P., "Subgrid-Scale Models for Large-Eddy Simulations of Compressible Wall Bounded Flows," *AIAA Journal*, Vol. 38, No. 8, 2000, pp. 1340–1350.

S. Mahalingham
Associate Editor

Accuracy of Higher-Order Finite Difference Schemes on Nonuniform Grids

Yongmann M. Chung* and Paul G. Tucker†
University of Warwick,
Coventry, England CV4 7AL, United Kingdom

I. Introduction

HIGHER-ORDER finite difference schemes are often used in the discretization of the spatial derivatives in transitional and turbulent flow simulations. A family of symmetric compact finite difference schemes with spectral-like resolution is developed by Lele.[1] The compact schemes have small computational stencil compared to other finite difference schemes of the same order. Hence, they are widely used for computational fluid dynamics and computational acoustics.[2–4] When higher-order finite difference schemes are used in computational fluid dynamics, there are two key issues encountered: boundary treatments and grid nonuniformity. The former aspect is addressed by several researchers.[5–7] Adams[7] concludes that its contribution of boundary schemes to overall resolution is small. The latter is the topic of the present study.

In turbulent flow simulations many flowfields are inhomogeneous in one or more directions. Because of the nature of turbulent flows and computing resource limitations, the use of nonuniform grid simulations is inevitable. In a typical direct numerical simulation (DNS) or large-eddy simulation (LES) of a wall-bounded flow,[8] the ratio of the maximum to the minimum grid spacing is about 100. The grid nonuniformity issue is important, and in this study we assess the accuracy of higher-order finite difference schemes on nonuniform grids. The following three higher-order finite difference schemes are considered: a sixth-order compact scheme (COM6), the standard Padé scheme (PADE), and the fourth-order central difference scheme (CEN4). The commonly used second-order central difference scheme (CEN2) is also included, as it has proven useful for DNS[9] and LES.[10] Scheme accuracies are compared using Fourier error analysis.

Received 24 December 2002; revision received 4 April 2003; accepted for publication 9 April 2003.

*Postdoctoral Researcher, Fluid Dynamics Research Centre, Department of Engineering; currently Lecturer, Department of Engineering and Centre for Scientific Computing; Y.M.Chung@warwick.ac.uk.

†Senior Lecturer, Fluid Dynamics Research Centre, Department of Engineering. Member AIAA.

II. Higher-Order Finite Difference Schemes

We can define an approximation to the first and second derivatives for the x direction of the values of $f(x)$ on the uniformly distributed grids $x_i = (x_1, \ldots, x_N)$ by $\boldsymbol{L}_1 f_i' = \boldsymbol{R}_1 f_i$ and $\boldsymbol{L}_2 f_i'' = \boldsymbol{R}_2 f_i$, where the operations of matrices $\boldsymbol{L}_1^{-1}\boldsymbol{R}_1$ and $\boldsymbol{L}_2^{-1}\boldsymbol{R}_2$ are the first and second derivative discrete projection operators, respectively. The quadratic matrices $\boldsymbol{L}_1$, $\boldsymbol{R}_1$, $\boldsymbol{L}_2$, and $\boldsymbol{R}_2$ can be determined from the numerical scheme.[1]

Following Lele,[1] the finite difference approximation f_i' to the first derivative $\mathrm{d}f/\mathrm{d}x$ at the node i can be obtained as follows:

$$\alpha f_{i-1}' + f_i' + \alpha f_{i+1}' = a\frac{f_{i+1} - f_{i-1}}{2\Delta x} + b\frac{f_{i+2} - f_{i-2}}{4\Delta x} \tag{1}$$

Only the tridiagonal schemes of $\boldsymbol{L}_1$ and $\boldsymbol{L}_2$ are considered. The relation between the coefficients are obtained by matching the Taylor-series coefficients of various orders and shown in Table 1 (see also Ref. 1).

In this study we restrict our interest to smoothly varying grids where there exists a mapping function that maps uniform grid in computational (ξ) space to the nonuniform grid in physical (x) space. Two type of nonuniform grid that are commonly used in DNS and LES are considered:

$$x = \frac{\sinh(\gamma\xi)}{\sinh(\gamma)} \tag{2}$$

$$x = \frac{\tanh(\gamma\xi)}{\tanh(\gamma)} \tag{3}$$

where γ is the control parameter. The former is adequate for free shear flows such as mixing layers,[2,3] whereas the latter has been widely used in the simulation of wall-bounded flows such as channel and pipe flows.[9] Three values of γ used here are 1.0, 2.0, and 3.0. In a typical channel flow DNS,[8,9] $\Delta y^+_{\max}/\Delta y^+_{\min} \approx 100$. This is similar to the $\gamma = 3$ case. Then, the first and second derivatives of a function $f(x)$ on nonuniform grids are evaluated as

$$\frac{\partial f}{\partial x} = \frac{1}{x_\xi}\frac{\partial f}{\partial \xi} \tag{4}$$

$$\frac{\partial^2 f}{\partial x^2} = \frac{1}{x_\xi^2}\frac{\partial^2 f}{\partial \xi^2} - \frac{x_{\xi\xi}}{x_\xi^2}\frac{\partial f}{\partial \xi} \tag{5}$$

III. Results and Discussion

A. Modified Wave Numbers

Fourier analysis of differencing errors is performed. This investigation closely follows that of Lele.[1] The finite difference equation (1) is of a central difference. Because of symmetry, compact schemes on uniform grid always have real wave numbers; hence, they contain no dissipation errors. However, the grid nonuniformity destroys this property, and the modified wave numbers become complex valued on nonuniform grids. The real part is related to dispersion errors and the imaginary part to dissipation errors. Modified wave numbers for each scheme are examined for two grid numbers ($N = 256$ and 32).

Table 1 Efficiency $e_1(\epsilon)$ and $e_2(\epsilon)$ of the schemes for $\varepsilon = 0.1$

	First derivative				Second derivative			
Scheme	α	a	b	$e_1(\epsilon)$	α	a	b	$e_2(\epsilon)$
COM6	1/3	14/9	1/9	0.70	2/11	12/11	3/11	0.80
PADE	1/4	3/2	0	0.59	1/10	6/5	0	0.68
CEN4	0	4/3	−1/3	0.44	0	4/3	−1/3	0.59
CEN2	0	1	0	0.25	0	1	0	0.35

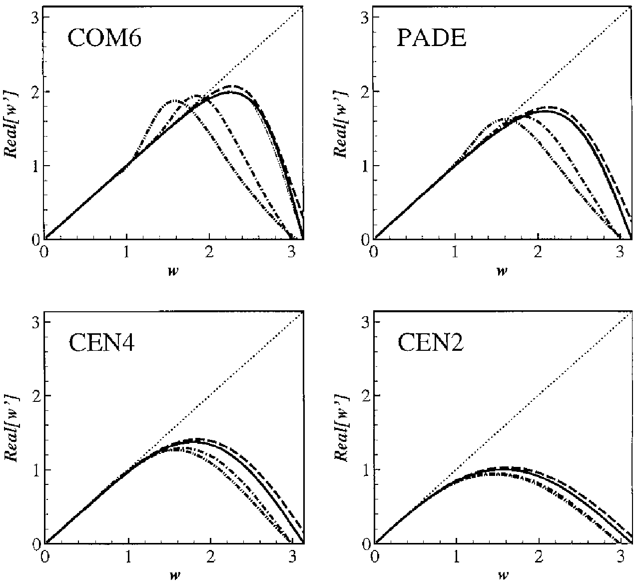

Fig. 1 Real part of the modified wave number for first derivative approximations on tanh grids: ——, uniform grid; - - -, tanh1 grid; -·-, tanh2 grid; -··-, tanh3 grid; · · · ·, SPEC; ▬▬, $N = 32$; and ——, $N = 256$.

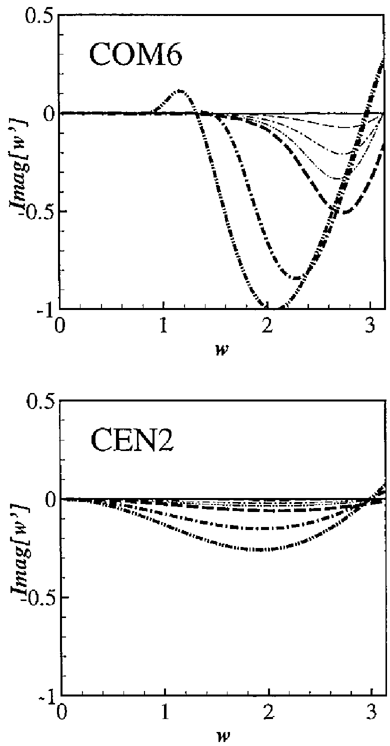

Fig. 2 Imaginary part of the modified wave number for first derivative approximations on tanh grids. See caption of Fig. 1.

Plots of real and imaginary parts of w' against w are presented in Figs. 1 and 2, respectively, on tanh grids. For reference w' from a spectral scheme (SPEC) is also included.

On uniform grid the advantage of using higher-order finite difference schemes over CEN2 is clear. To compare scheme accuracies quantitatively, as proposed by Lele,[1] efficiency parameters are introduced. The useful region, where the modified wave number is close to the spectral value, is much larger in the higher-order schemes (see Table 1). As the grid nonuniformity increases, the modified wave number w' is affected significantly. The dissipation errors increase substantially. The schemes tested here contain no dissipation errors on the uniform grid. The deterioration of accuracy is serious for the higher-order schemes. The deviation of w' from their uniform grid values becomes much larger on course grids. Overshoots in w'

Table 2 Resolved fraction for 10% error in modified wave number w' with $N = 256$

		Sinh grids			Tanh grids		
Scheme	Uniform	$\gamma = 1$	$\gamma = 2$	$\gamma = 3$	$\gamma = 1$	$\gamma = 2$	$\gamma = 3$
COM6	0.73	0.67	0.48	0.38	0.63	0.44	0.34
PADE	0.66	0.62	0.47	0.37	0.58	0.42	0.33
CEN4	0.54	0.52	0.42	0.35	0.49	0.38	0.31
CEN2	0.41	0.41	0.36	0.32	0.39	0.34	0.29

Table 3 Resolved fraction for 10% error in modified wave number w'' with $N = 256$

		Sinh grids			Tanh grids		
Scheme	Uniform	$\gamma = 1$	$\gamma = 2$	$\gamma = 3$	$\gamma = 1$	$\gamma = 2$	$\gamma = 3$
COM6	0.87	0.82	0.67	0.58	0.79	0.62	0.53
PADE	0.79	0.77	0.65	0.57	0.74	0.61	0.52
CEN4	0.74	0.72	0.63	0.56	0.70	0.59	0.52
CEN2	0.62	0.62	0.58	0.54	0.60	0.54	0.50

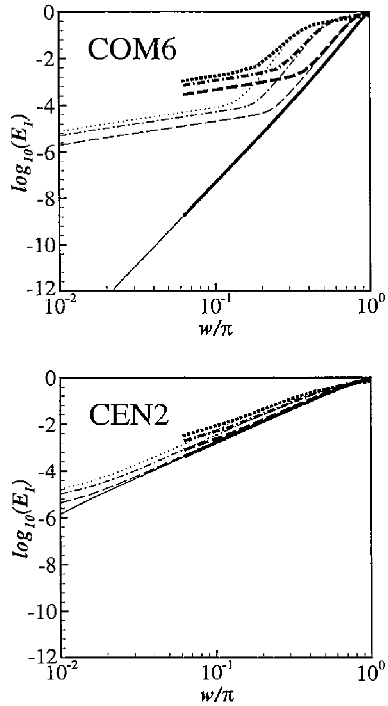

Fig. 3 Errors of the finite difference schemes on tanh grids: ——, uniform grid; - - -, tanh1 grid; -·-, tanh2 grid; · · · ·, tanh3 grid; ▬▬, $N = 32$; and ——, $N = 256$.

are seen for COM6 and PADE in Fig. 1. For the CEN4 and CEN2 cases, relative to the compact schemes (COM6 and PADE), the effects of grid nonuniformity on w' are small. Especially in CEN2, the changes in w' remains small for all types of grids tested. Similar features are observed on sinh grids.

B. Errors of Finite Difference Schemes

Figure 3 shows finite difference scheme errors on the tanh grids. Because w' is a function of x on a nonuniform grid, the global l_2-norm error is analyzed.

$$E_1 = \|w'(w) - w\| \tag{6}$$

$$E_2 = \|w''(w) - w^2\| \tag{7}$$

Uniform grid results are also included using solid lines. In comparing the nonuniform results, the most obvious difference is the rate of convergence at small w. On a uniform grid these curves asymptotically approach zero according to their theoretical convergence rate.[5] On nonuniform grids the error of each scheme decreases following its theoretical convergence rate only for $E_1 \geq 10^{-4}$. Below this value the error is dominated by the grid nonuniformity [see Eq. (5)], and each scheme shows similar behavior. For a course grid ($N = 32$) the change occurs at a higher value of E_1. E_2 also shows similar behavior (not shown here).

Another property of the approximate operators is the behavior of the error at large w. This is important because it determines the range of spatial scales that can be resolved by the numerical scheme.[5] In Tables 2 and 3 the resolved fraction for 10% error in w' and w'' is listed, respectively, for the numerical schemes tested. It can clearly be seen that for stretched grids the spectral-like accuracy of the compact finite difference schemes has not been maintained. For all schemes tested, the magnitude of errors is increased substantially. It is also found that the higher the scheme order, the larger the error grows. In COM6 and PADE the accuracy decreases substantially at $\gamma = 3$. However, grid nonuniformity decreases the 10% resolved fraction of CEN2 only marginally. Therefore, as the grid nonuniformity increases ($\gamma = 3$) the benefit of using higher-order schemes almost disappears. Unlike the higher-order schemes, CEN2 error is not greatly affected by grid nonuniformity.

IV. Conclusions

The accuracy of higher-order finite difference schemes on a nonuniform grid is investigated. Four finite difference schemes that are widely used in DNS and LES are considered: a sixth-order compact scheme (COM6), the standard Padé scheme (PADE), the fourth-order central difference (CEN4), and the second-order central difference (CEN2). Two types of nonuniform grid are tested: hyperbolic-sine and hyperbolic-tangent grids. The grid quality has stronger effects on the higher-order compact schemes than on CEN4 and CEN2. It is found that CEN2 scheme is highly insensitive to grid quality, justifying its popularity in engineering computational fluid dynamics. The accuracy deterioration of higher-order compact schemes with low grid density is observed. Unlike CEN2, such schemes use broad information to evaluate derivatives. Consequently, higher-order schemes are more sensitive to grid quality. Although we considered two types of nonuniform grid, the findings of the present work can be generally extended to nonuniform grids where we can find a smooth mapping function.

Acknowledgment

The support of the Engineering and Physical Sciences Research Council of the United Kingdom under Grant GR/N05581 is gratefully acknowledged.

References

[1]Lele, S. K., "Compact Finite Difference Schemes with Spectral-Like Resolution," *Journal of Computational Physics*, Vol. 103, 1992, pp. 16–42.

[2]Sandham, N. D., and Reynolds, W. C., "Three Dimensional Simulations of Large Eddies in the Compressible Mixing Layer," *Journal of Fluid Mechanics*, Vol. 224, 1991, p. 133.

[3]Chung, Y. M., Luo, K. H., and Sandham, N. D., "Direct Numerical Simulation of an Impinging Jet," *International Journal of Heat and Fluid Flow*, Vol. 23, No. 5, 2002, pp. 592–600.

[4]Kim, J. W., and Lee, D. J., "Optimized Compact Finite Difference Schemes with Maximum Resolution," *AIAA Journal*, Vol. 34, No. 5, 1996, pp. 887–893.

[5]Kwok, W. Y., Moser, R. D., and Jiménez, J., "A Critical Evaluation of the Resolution Properties of B-Spline and Compact Finite Difference Methods," *Journal of Computational Physics*, Vol. 174, 2001, pp. 510–551.

[6]Carpenter, M. H., Gottlieb, D., and Abarbanel, S., "The Stability of Numerical Boundary Treatments for Compact High-Order Finite-Difference Schemes," *Journal of Computational Physics*, Vol. 108, 1993, p. 272.

[7]Adams, N. A., "Direct Numerical Simulation of Turbulent Compression Ramp Flow," *Theoretical and Computational Fluid Dynamics*, Vol. 12, 1998, pp. 109–129.

[8]Kim, J., Moin, P., and Moser, M., "Turbulent Statistics in Fully Developed Channel Flow at Low Reynolds Number," *Journal of Fluid Mechanics*, Vol. 177, 1987, p. 133.

[9]Chung, Y. M., and Sung, H. J., "Initial Relaxation of Spatially Evolving Turbulent Channel Flow with Blowing and Suction," *AIAA Journal*, Vol. 39, No. 11, 2001, pp. 2091–2099.

[10]Yang, K. S., and Ferziger, J. H., "Large-Eddy Simulation of Turbulent Obstacle Flow Using a Dynamic Subgrid-Scale Model," *AIAA Journal*, Vol. 31, 1993, p. 1406.

R. M. C. So
Associate Editor

Vibration–Dissociation Coupling Model for Hypersonic Blunt-Body Flow

Eswar Josyula*
U.S. Air Force Research Laboratory,
Wright–Patterson Air Force Base, Ohio 45433
and
William F. Bailey†
U.S. Air Force Institute of Technology,
Wright–Patterson Air Force Base, Ohio 45433

Nomenclature

k	=	Boltzmann constant
L	=	last vibrational level
M	=	Mach number, molecular weight
T	=	translational temperature
T_v	=	vibrational temperature for which population densities correspond to a Boltzmann distribution
v, w	=	vibrational quantum numbers
x, y	=	Cartesian coordinates
Γ_v	=	equilibrium fractional population in state v
ϵ	=	quantum level energy
ρ_s	=	density of species s
ρ_v	=	state density in the vth vibrational level
φ_L	=	deviation of last vibrational level, the dissociating state
φ_v	=	deviation of quasisteady distribution from an equilibrium Boltzmann distribution

Subscripts

i, j	=	species indices in quantum levels v, w
s	=	species O_2, N_2, O, N
v	=	vibrational level

Introduction

THE kinetics of thermal dissociation has long been a topic of theoretical research because of the difficulty of reconciling the measured rates. Current kinetic processes associated with reconciling the disparity include depletion effects from the upper vibrational levels and possible effects of rotational energy on the dissociation mechanism. Early attempts by Hammerling et al.[1] to model vibration–dissociation coupling (CVD) used a simple harmonic oscillator assumption for the vibrational energy resulting in the vibrational population relaxing through a sequence of Boltzmann distributions. The coupled vibration–dissociation (CVDV) model of Treanor and Marrone[2] extended the CVD model to account for

Presented as Paper 2001-2733 at the AIAA 32nd Plasmadynamics and Lasers Conference, Anaheim, CA, 11–14 June 2001; received 3 October 2001; revision received 10 April 2003; accepted for publication 21 April 2003.

*Research Aerospace Engineer, AFRL/VAAC, 2210 Eighth Street. Associate Fellow AIAA.

†Associate Professor, AFIT/ENP, 2950 P Street.